

# **A Comparative Analysis of Fourier Transform And Wavelet Transform in Denoising Photoplethysmographic Signal Towards Stress Detection**

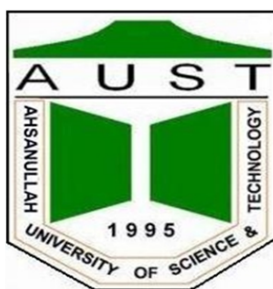
**Thesis & Project-I  
CSE 4100**

A thesis Report  
Submitted in partial fulfillment of the requirements for the Degree of  
Bachelor of Science in Computer Science and Engineering

Submitted By

|                        |                  |
|------------------------|------------------|
| <b>Tahlamuna Rulpi</b> | <b>170204083</b> |
| <b>Jesmin Akter</b>    | <b>180104052</b> |
| <b>Ramisa Maliyat</b>  | <b>180104079</b> |
| <b>Sadia Sultana</b>   | <b>180104094</b> |

Supervised By  
**Md. Aminur Rahman**  
Assistant Professor  
Department of CSE  
Ahsanullah University of Science and Technology



**Department of Computer Science and Engineering  
Ahsanullah University of Science and Technology  
Dhaka, Bangladesh**

June 26,2022

## Abstract

Stress and mental health have become major concerns worldwide. Chronic stress could implicate several psychophysiological disorders. For example, stress increases the likelihood of depression, stroke, heart attack, and cardiac arrest. In recent years the focus of the field has shifted from the laboratory to the real life environment. Signals can be collected through wearable devices to measure stress. These devices can be attached to the chest, head or wrist etc. If sensors are attached to the wrist, it is simpler and more convenient in everyday life. But these signals are affected by many internal and external noises. Also for ubiquitous and real-time measurement systems, signals are easily prone to motion artifacts (MA) which could lead to inaccurate results. Our aim is to compare between several denoising methods to improve stress detection performance. We have used a public dataset namely, wearable stress and affect detection dataset (WESAD). From this dataset, we got photoplethysmogram (PPG) data. By applying a two step denoising method with fourier transform and ensemble based peak detection on that signal an improved result compared to the paper that introduces WESAD can be achieved. In future, we will implement wavelet transform instead of fourier transform to see whether it performs better or not.

**Keywords:** Stress, Physiological signals, Wearable devices, Photoplethysmogram, Fourier transform, Wavelet transform

# Table of Contents

|   |            |
|---|------------|
| <b>Abstract</b>   | <b>i</b>   |
| <b>Table of Contents</b>                                      | <b>ii</b>  |
| <b>List of Figures</b>  | <b>iii</b> |
| <br>  |            |
| <b>1 Introduction</b>   | <b>1</b>   |
| 1.1 Introduction . . . . .                                    | 1          |
| 1.2 Motivation . . . . .                                      | 1          |
| 1.3 Objective . . . . .                                       | 2          |
| 1.4 Thesis Organization . . . . .                             | 2          |
| <br>  |            |
| <b>2 Literature Review</b>                                    | <b>3</b>   |
| 2.1 Transformation techniques in Signal Processing: . . . . . | 3          |
| 2.2 Related works . . . . .                                   | 6          |
| <br>  |            |
| <b>3 Methodology</b>  | <b>8</b>   |
| 3.1 Dataset And Attributes . . . . .                          | 8          |
| 3.2 Two step denoising method . . . . .                       | 9          |
| 3.3 Ensemble-based peak detection method . . . . .            | 10         |
| 3.4 Feature extraction . . . . .                              | 10         |
| <br>  |            |
| <b>4 Experimental Result</b>                                  | <b>13</b>  |
| 4.1 Experimental setup . . . . .                              | 13         |
| 4.2 Integrated Approach Performance . . . . .                 | 13         |
| 4.3 Two-Step denoising method performance . . . . .           | 15         |
| 4.4 Ensemble-based peak detection performance . . . . .       | 16         |
| <br>  |            |
| <b>5 Conclusion And Future work</b>                           | <b>17</b>  |
| 5.1 Conclusion . . . . .                                      | 17         |
| 5.2 Future Work . . . . .                                     | 17         |
| <br>  |            |
| <b>References</b>   | <b>18</b>  |

# List of Figures

|     |   |    |
|-----|---|----|
| 2.1 | Applying Fourier series on a cycle-by-cycle basis                             | 4  |
| 2.2 | Flowchart for denoising signals using Fourier transform.                      | 5  |
| 2.3 | Fourier analysis and data reconstruction                                      | 6  |
| 3.1 | Entire process of the work  | 8  |
| 4.1 | Performance results of the methods  | 13 |
| 4.2 | Performance of two-step denoising method with ensembled peak detection method | 15 |

# Chapter 1

## Introduction

### 1.1 Introduction

Measuring stress accurately has become a crucial task for people. In the past, stress was measured by using a survey. Nowadays, Wearable sensors are used for measuring physiological signals to detect stress. Electrocardiogram (ECG) and Photoplethysmogram (PPG) signals are commonly used for stress detection. PPG signal is used to estimate the blood flow of the body and detect volumetric changes in blood in the peripheral circulation. It is a non-invasive technology that uses a light source and a photodetector at the surface of the skin that is used to measure variations in blood circulation. PPG data are collected by attaching sensors with wrist devices. For this reason, the devices become more convenient and reliable, and cost-effective. The denoising technique of PPG signals is the procedure to separate noisy or corrupted signals from the original signal. Denoising techniques are performed in terms of time and frequency. Recent methods for peak detection focus on the non-systolic peak, especially the peak that is triggered by noise. In our research work, we have detected peaks by extracting the peak with the largest amplitude value and using signal transformation and thresholding to reduce non-systolic peaks. We have used orchestrating multiple denoising and peak-detecting methods to improve the performance of stress detection and overcome the limitations of previous PPG signal analysis.

### 1.2 Motivation

In our daily life, stress is a very common word that we use. When we have lots of responsibilities that we are struggling to manage then we may feel stressed. Sometimes, a small amount of stress can help us to complete tasks and feel more energized which is called acute stress which happens within a few minutes to a few hours of an event. But stress can become a problem when it lasts for a long time or is very intense which is called chronic stress that keeps coming back. In some cases, stress can affect our physical and mental health. And it can make existing problems worse. Being able to recognize common stress symptoms can help us manage them. Stress that's left unchecked can contribute to many health problems, such as high blood pressure, chest pain, heart disease, obesity and diabetes. These critical issues motivated us to work on this topic which may help people to be careful of their health before unwanted things happen. It also helps people to overcome stress by taking proper measures in time. PPG devices are now widely used because it is convenient, low-powered, cheap and also easy to handle due to its small size. Hence we choose to process this signal.

## 1.3 Objective

In our research, our aim is to improve stress detection performance. For stress detection, Signals can be collected through wearable devices such as chest, head or wrist devices etc. If we use this signal after reducing the noise, it provides a better result than using the signal with noise. In this study, we will explore which method between Fourier transform and wavelet transform performs better on PPG signals to reduce noise. PPG is a signal that represents a changing arterial wave during each cardiac cycle, and the data are collected by attaching sensors to the wrist. Therefore, setting up devices is inexpensive and convenient. In this research paper, we have used a public dataset (WESAD) which provides various types of physiological signals and is labeled with four emotional states: baseline, stress, amusement, and meditation, which is full of all related information.

## 1.4 Thesis Organization

In our research, our main aim is to see which denoising method performs better to reduce noise from PPG signals.

Chapter 1 (Introduction): In this chapter, we have discussed problem definition, basic concepts and our aim to use Machine learning (ML) to detect stress.

Chapter 2 (Literature Review): In this chapter, we have discussed a short description of related papers which we have studied. We have also explained our transformation techniques here.

Chapter 3 (Methodology): In this chapter, we have discussed our techniques for denoising PPG signals to detect stress, and peak detection methods. We have also explained our work ideas and features. We have discussed the WESAD dataset here.

Chapter 4 (Experimental Result): In this chapter, we have discussed our experimental setup and results.

Chapter 5 (Conclusion And Future work): Here we have finished up our paper by featuring our topic. Probable future plans and ideas are also described here.

# Chapter 2

## Literature Review

### 2.1 Transformation techniques in Signal Processing:

The Fourier transformation is a mathematical formula that is a translation between two mathematical worlds: Signals and Frequency which relates a signal sampled in time or space to the same signal sampled in frequency.

Cycle-by-cycle Fourier series analysis is used to extract clean PPG from PPG signals corrupted by motion artifacts.[6]

Let,  $f(t)$  represent the periodic signal with the  $T$  period.

Fourier series will be,  $f(t) = a_0 + \sum_{k=1}^{\infty} a_k \cos(kwt) + b_k \sin(kwt) \dots\dots(1)$  where

$$w = \frac{2\pi}{T} \dots\dots(2)$$

$$a_0 = \frac{1}{T} \int_0^T f(t) dt \dots\dots(3)$$

$$a_k = \frac{2}{T} \int_0^T f(t) \cos(kwt) dt \dots\dots(4)$$

$$b_k = \frac{2}{T} \int_0^T f(t) \sin(kwt) dt \dots\dots(5) \quad [6]$$

Fourier transformation cannot be directly applied to a PPG signal. By applying the cycle by cycle Fourier series the problem is solved. Now,

$$f_c(t) = f(t) + f_a(t)$$

Where  $f_c(t)$  represents the resultant corrupted PPG signal

$f(t)$  is the original artifact-free PPG signal

$f_a(t)$  is the motion artifact.

Compute the Fourier series coefficients of the  $m$ th cycle, we get,

$$ma_{0c} = \frac{1}{T_m} \int_0^{T_m} f_c(t) dt = \frac{1}{T_m} \int_0^{T_m} [f(t) + f_a(t)] dt$$

$$= {}_m a_0 + \frac{1}{T_m} \int_0^{T_m} f_a(t) dt \dots\dots(8)$$

$${}_m a_{kc} = {}_m a_k + \frac{2}{T_m} \int_0^{T_m} f_a(t) \cos(kw_m t) dt \dots\dots(9)$$

$${}_m b_{kc} = {}_m b_k + \frac{2}{T_m} \int_0^{T_m} f_a(t) \sin(kw_m t) dt \dots\dots(10)$$

Here,  $(\frac{2}{T_m}) \int_0^{T_m} f_a(t) \cos(kw_m t) dt$  and  $(\frac{2}{T_m}) \int_0^{T_m} f_a(t) \sin(kw_m t) dt$  individually would evaluate to zero, which means PPG is not correlated with motion artifacts. Applying this condition, we get,

$${}_m a_{kc} = {}_m a_k \text{ and}$$

$${}_m b_{kc} = {}_m b_k$$

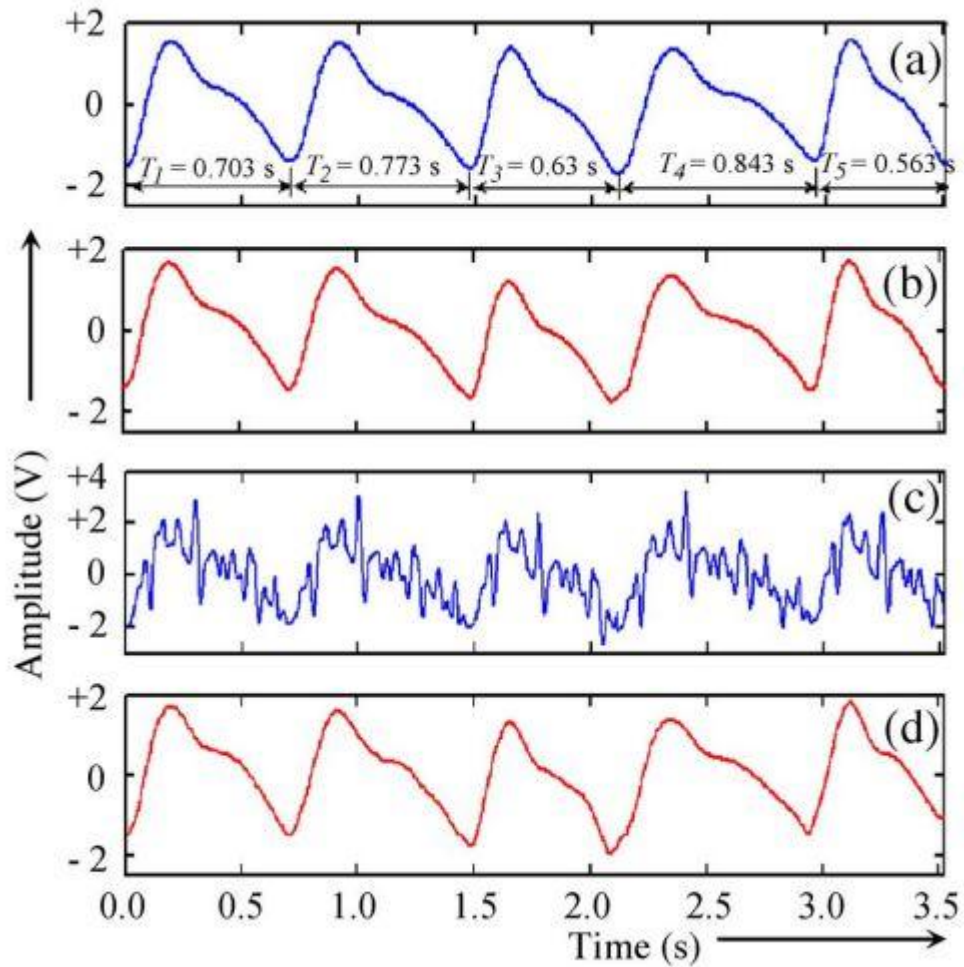


Figure 2.1: Applying Fourier series on a cycle-by-cycle basis [6]



In figure 2.1(a), a motion artifact is intentionally added with the original noise-free signal. In figure 2.1(b) PPG extracted from (a) with only the first seven Fourier coefficients. In figure 2.1(c), the resultant corrupted PPG signal is shown. Figure 2.1(d) clearly shows that Fourier transformation extracts clean PPG signal from corrupted PPG signal by motion artifact.

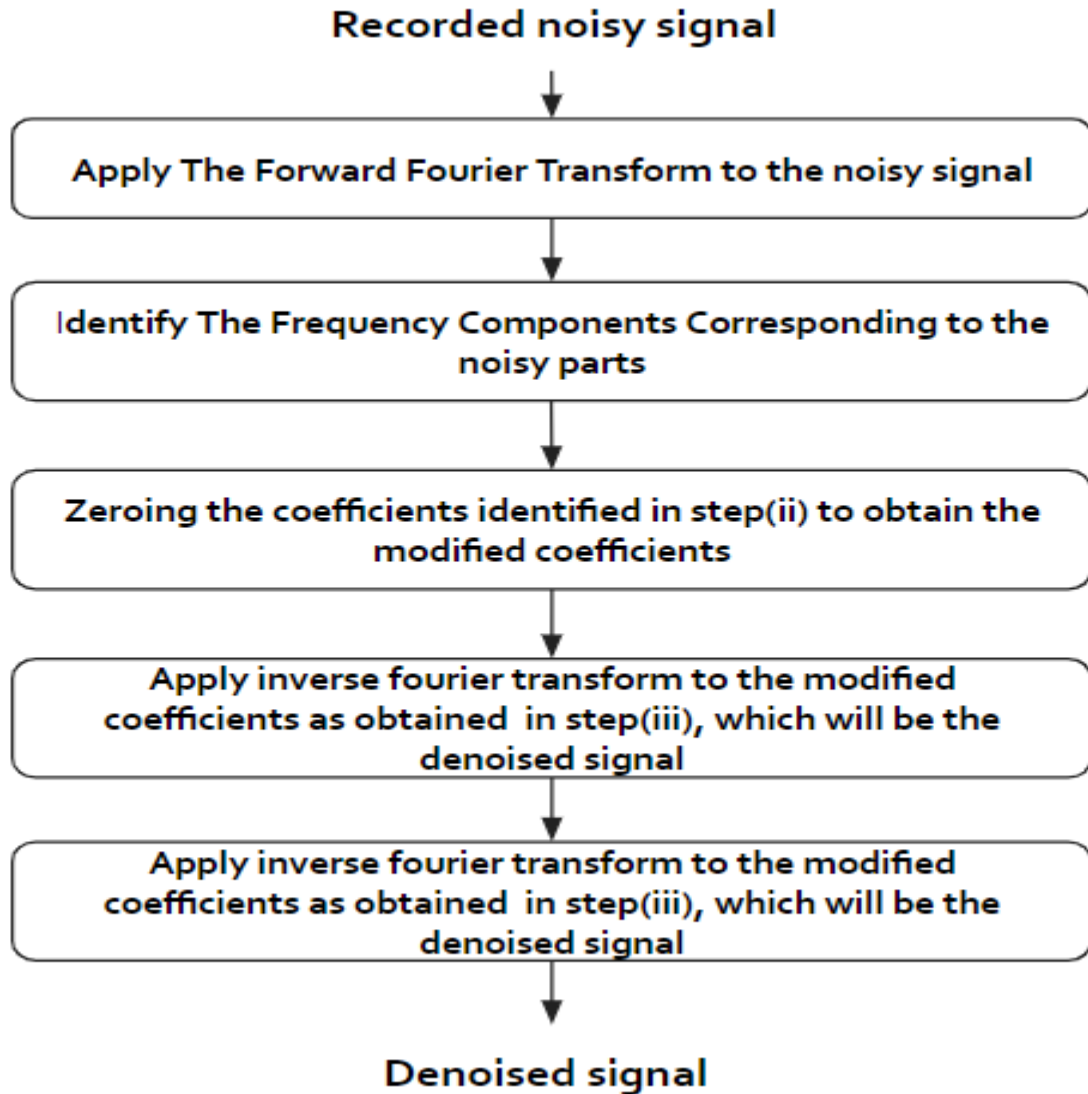


Figure 2.2: Flowchart for denoising signals using Fourier transform[12]

Fourier transform (FT) is used to analyze the behavior of PPG signals in the frequency domain. The signal is first transformed into the frequency domain by a fast Fourier transform (FFT). After being transformed, the basic frequency of the PPG signal is used to detect peak values. The signal is reconstructed by an inverse Fourier transform taking first and second harmonics. [13]

In figure 2.3, the first row represents the recorded signal in the time domain. Here, the red line indicates the waveform of 660nm and the blue line is the waveform of 870 nm. The second row

shows the transformed signals in the frequency domain. The third row is the reconstructed signal.

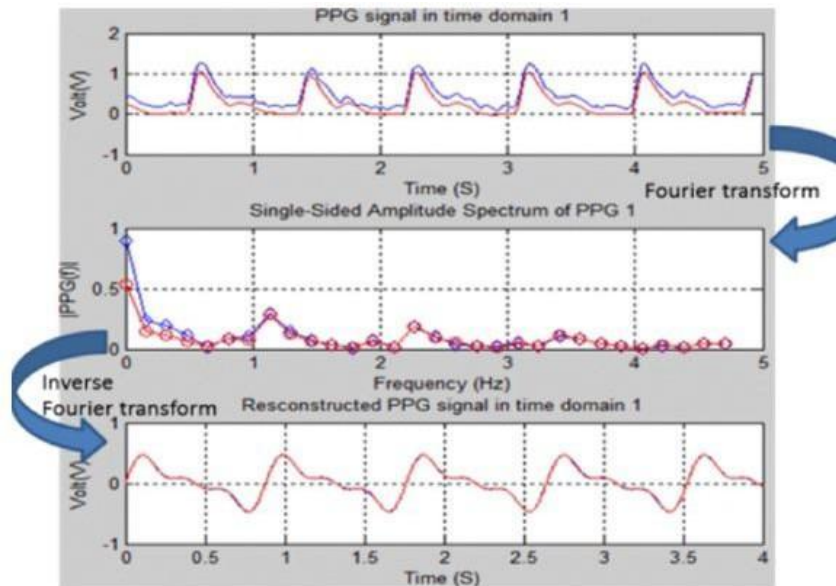


Figure 2.3: Fourier analysis and data reconstruction [13]

Wavelet transformations work in both the time and frequency domains simultaneously. In general, in pure periodic signals, the period is constant irrespective of time. So, in analyzing the quasi-periodic signals the Fourier transform is not adequate. Wavelet transformation provides a viable solution because they are useful for examining aperiodic, noisy signals. [12]

## 2.2 Related works

B. Mishra and N. S. Nirala [3] This is a survey paper on different denoising techniques for PPG signals. The denoising technique of PPG signal is the procedure of separation of corrupted or noisy signals from the original signal. PPG signals are usually affected by different artifacts. Power line Interface, Motion Artifact (MA), Low amplitude PPG signal, premature Ventricular Contraction, and Baseline Wander (BW) are different types of noises that corrupt the signal. To eliminate noise special filters have been used such as LMS filter, moving average filter, adaptive filters, Kalman filter, IMAR, Wavelets, median filter, notch filter, etc.

S. S. Bashar, M. S. Miah, A. H. M. Z. Karim and M. A. Al Mahmud [15] In this paper, a Machine Learning Approach using Decision Tree Regression Algorithm: Photoplethysmography (PPG) signal has been used to measure heart rate. In this research paper, a multi-model machine learning approach (MMMLA) is applied to predict heart rate from wearable devices such as fingertip devices, and wrist-type devices. In this technique, K means clustering has been used for splitting noisy and non-noisy data. After splitting, the separated data has been used to fit into the Decision Tree regression framework and measured the heart rate for test data. In this

research, feature engineering has also been done. In feature engineering, a set of features have been chosen and checked the behavior with different models.

Islam, M.T., Ahmed, S.T., Shahnaz, C. et al. [16] To remove motion artifacts from the PPG signal, a fast algorithm for heart rate estimation based on a modified spectral subtraction scheme utilizing Composite Motion Artifacts Reference generation (SPECMAR) with two-channel PPG and three-axis accelerometer signals has been proposed in this paper. The motion artifact is captured by taking the minimum amplitude of each of the frequency bins of the three-channel accelerometer. Using this technique, an accurate heart rate is estimated so that significant noise reduction is achieved. SPECMAR method is capable of tracking the ground truth with high estimation accuracy. Therefore, it can be used in real-time applications without giving up estimation accuracy. Due to low computational complexity, the method is relatively faster than other methods. SPECMAR method is implemented in wearable devices because of the low estimation error, and smooth and fast heart rate tracking.

D. Ban and S. Kwon [17] This research paper proposed a movement noise cancellation algorithm for PPG signals using multipath diversity and the wavelet transform. Multi-path diversity of PPG signals has been measured at different locations on the body, such as fingers and eyes. After measuring the PPG signals, the wavelet transform has been used to detect movement noise in the signals. Although high-frequency noise can be filtered out using a low pass filter movement noise cannot be canceled by a low pass filter because a nominal pulsatile has frequencies lower than 4 Hz.

A. Alqaraawi, A. Alwosheel, and A. Alasaad [8] This research paper proposed a probabilistic approach based on Bayesian learning. This technique is used to estimate HRV from PPG signals recorded by wearable devices. The automatic multi-scale-based peak detection (AMPD) algorithm has been used to enhance the performance of peak detection in terms of sensitivity and positive predictive values. This algorithm aims to detect signal peaks by analyzing the local maxima scalogram (LMS) of periodic or quasi-periodic signals.

K. A. Reddy, B. George and V. J. Kumar [6] In this paper, Fourier series analysis has been used to reduce the effect of motion artifacts on pulse oximeter reading. When the patient is connected to the oximeter, oxygen saturation ( $SpO_2$ ) is measured. Cycle-by-cycle Fourier series analysis has been used to extract clean PPG from PPG signals corrupted by motion artifacts.

K. V. P. Naraharisetti and M. Bawa [18] In this paper, researchers have shown a comparison of different signal processing methods including Adaptive Noise Cancellation (ANC), Wavelet Transform (WT), Independent Component Analysis (ICA), Singular Value Decomposition (SVD), and Cycle by Cycle Fourier series Analysis (FSA) which have been implemented toward motion artifact reduction. After implementing the five methods, they have concluded that SVD and FSA methods give better results in terms of artifact reduction.

# Chapter 3

## Methodology

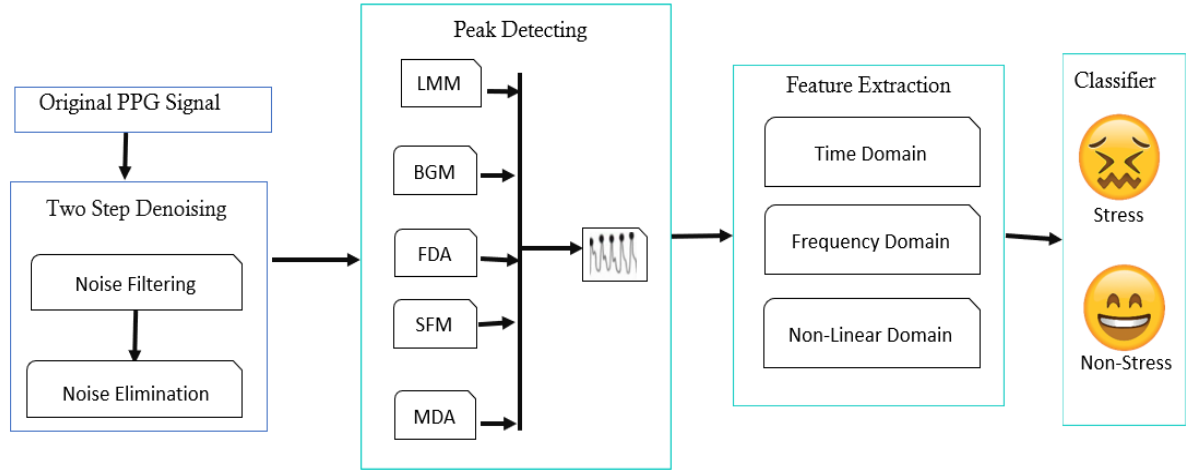


Figure:3.1 Entire process of the work

Our approach consists of denoising, peak detection, and feature extraction. We use 7 lightweight classifiers which are available on low-power wearable devices to measure performance on stress detection. Figure 3.1 shows the overall process of our work.

### 3.1 Dataset And Attributes

Long-term stress is known to have severe implications on wellbeing, which call for continuous and automated stress monitoring systems. The affective computing community lacks commonly used standard datasets to detect a person's affective state based on observables. Therefore, we have used WESAD, a publicly available dataset for wearable stress and affect detection. This multimodal dataset features physiological and motion data, recorded from both a wrist and a chest-worn device, of 15 subjects during a lab study. The following sensor modalities are included: blood volume pulse(BVP), electrocardiogram(ECG), electrodermal activity(EDA), electromyogram(EMG), respiration(RESPIR), body temperature(TEMP), and three-axis acceleration(ACC). Hence attributes of this dataset are BVP, ECG, EDA, EMG, RESPIR, TEMP, and ACC. In addition, self-reports of the subjects, which were obtained using several established questionnaires, are contained in the dataset. In this dataset, by considering the three-class classification problem (baseline vs. stress vs. amusement), they achieved classification accuracies of up to 80%. In the binary case (stress vs. non-stress), accuracies of up to 93% were reached. In our experiments, only the PPG signal was used.

### 3.2 Two step denoising method

PPG signal denoising process contains two steps:

- Noise filtering
- Noise elimination

In the noise filtering step, We use the Band-pass filter and Moving average filter. The band-pass filter is used to compensate for the signal in terms of frequency and the Moving average filter for signal smoothing.

In the noise elimination step, We have used a statistical method to remove noisy segments of signals in terms of time. At first, we extracted the valley from noisy signals and per cycle divided it into segments. The general moving-window method has an inaccurate valley-detection problem because due to noise all signals detect incorrect valleys continuously. To overcome this problem, we have calculated the mean of the entire signal amplitude and set segments from previous to the current points. Each segment contains mean values of the amplitude of the entire signal. We have calculated the standard derivation, kurtosis, and skewness of all segmented data using the following expressions:

$$\text{Standard deviation, } \sigma = \sqrt{\frac{1}{n} \sum_{i=0}^n (x_i - \bar{x})^2}$$

$$\text{Kurtosis} = \frac{\frac{1}{n} \sum_{i=1}^n (x_i - \bar{x})^4}{std^4}$$

$$\text{Skewness} = \frac{\frac{1}{n} \sum_{i=1}^n (x_i - \bar{x})^3}{std^3}$$

Here,  $\sigma$  stands for standard deviation and  $\bar{x}$  is for mean value.

We have calculated the threshold  $T_\sigma$ ,  $T_k$ , and  $T_{s1}$  using the following expression:

$$T_\sigma = \bar{\sigma} + \alpha \quad , \quad T_k = \bar{k} + \beta \quad \text{and}$$

$$T_{s1} = \bar{s} - \gamma \quad , \quad T_{s2} = \bar{s} + \delta$$

Here,  $\bar{\sigma}$ ,  $\bar{k}$ , and  $\bar{s}$  represents standard deviation, kurtosis, and skewness, respectively.

The values of optimal parameters are:

$$\alpha = 1.0, \beta = 2.0, \gamma = 1.8, \text{ and } \delta = 1.5.$$

Removing all the segments beyond the threshold, we have reconstructed the signal. Finally, for smoothing the final signal we have used a moving average filter.

### 3.3 Ensemble-based peak detection method

We have applied the ensemble to five peak-detecting methods e.g. LMM, BGM, FDA, SFA, MAD., and used majority voting to determine the final peak point.

**Local maxima method (LMM):** This method extracts all the local points from the signal and removes the points which have less value than the mean of the entire signal amplitude.

**Block generation with the mean of the signal threshold method (BGM):** This method generates the blocks with the mean values of the amplitude of the signal. The peak point contains the largest values of each block.

**First derivative with an adaptive threshold method (FDA):** Using this method, the signals are differentiated and the points with differential values of zero are considered peak candidates. Here, we have considered the peak point which peaks candidates with a larger amplitude than the threshold. We have set the threshold by applying a selective window of 2-sec duration at the beginning of each block.

**Slope sum function with an adaptive threshold method (SFA):** This method extracts all local points from the modified signal. For doing this, we have left only the ascending points throughout the entire differential process and set the remaining points with zero. We have extracted only the point with a larger amplitude than the threshold. The extracted peak points represent the final peak point of the modified signal. The main objective of the slope sum function is to enhance the upslope of the PPG pulse and to cover the remainder of the pressure waveform.

**Moving averages with the dynamic threshold method (MAD):** We have set signals below zero and taken the square of all signals. As a result, the block is generated by two moving averages. In each exerted block, the largest amplitude point has become the peak point.

### 3.4 Feature extraction

Table 3.1 : List of extracted features

| Domain | Parametrer | Description                   | Unit            |
|--------|------------|-------------------------------|-----------------|
|        | Mean HR    | Mean HR                       | $\frac{1}{min}$ |
|        | StdHR      | Standard deviation of the HRs | $\frac{1}{min}$ |
|        | MeanNN     | Mean of N-N intervals         | ms              |

|           |           |  |        |
|-----------|-----------|--|--------|
| Time      | SDNN      | Standard deviation of N-N intervals                                    | ms     |
|           | MedNN     | Median of N-N intervals  | ms     |
|           | MeanSD    | Mean of successive N-N interval differences                            | ms     |
|           | SDSD      | Standard deviation of successive N-N interval differences              | ms     |
|           | RMSSD     | Root mean square of successive N-N interval differences                | ms     |
|           | pNN20     | Percentage of successive N-N intervals that differ by more than 20ms   | %      |
|           | pNN50     | Percentage of successive N-N intervals that differ by more than 50ms   | %      |
|           | TINN      | Baseline width of the R-R interval histogram                           | M s    |
| Frequency | LF        | Power in the low-frequency band(0.04 - 0.15Hz)                         | $ms^2$ |
|           | HF        | Power in the high-frequency band(0.15 - 0.4Hz)                         | $ms^2$ |
|           | LF/HF     | Ratio of LF to HF  |        |
|           | ULF       | Power in the ultra-low-frequency band( $\leq$ 0.003Hz)                 | $ms^2$ |
|           | VLF       | Power in the very-low-frequency band(0.003 - 0.04Hz)                   | $ms^2$ |
|           | P(TotPow) | Total power 0.003-0.4Hz  | $ms^2$ |
|           | LF/P      | Ratio of low-frequency to total power                                  | -      |
|           | HF/P      | Ratio of high frequency to total power                                 | -      |
|           | SD1       | Poincare plot standard deviation perpendicular to the line of identity | M s    |

|            |        |  |        |
|------------|--------|--|--------|
| Non-Linear | SD2    | Poincaré plot standard deviation along the line of identity            | M s    |
|            | pQ     | $pQ = SD1 / SD2$   | -      |
|            | pA     | $pA = SD1 * SD2$   | $ms^2$ |
|            | ApEn   | Approximate entropy  | -      |
|            | ShanEn | Shannon entropy  | -      |
|            | D2     | Correlation dimension, which estimates the minimum number of variables | -      |

Heart rate variability (HRV) has become the indicator for various health and disease conditions. PPG sensors are widely used to measure heart activities. HRV requires an accurate estimation of the time interval between successive peaks in the PPG signal. To calculate HRV, the signal must be split up into accurate window sizes. At least two min window length is required to extract all the features accurately. To extract HRV features we have used 2 min of window length and 0.25 sec of the sliding window. All the peak points are not perfectly extracted so there exists an inaccurate interval between successive peaks. To solve this problem, we have eliminated approximately 300 ms greater or lesser than the mean of entire intervals, the rest used for HRV feature extraction. To extract the HRV feature, we have used the HRV time domain, frequency domain, and non-linear domain. The features we have used are listed in Table1.



# Chapter 4

## Experimental Result

### 4.1 Experimental setup

WESAD provides various types of physiological signals and is labeled with four emotional states: baseline, stress, amusement, and meditation[5]. The baseline condition represents a neutral affective state. We have used only a single PPG signal with a 64 Hz sampling rate. A 0.1% high-quality signal with high-peak-detection performance was extracted and used as a reference signal to set up the cut-off and threshold in the noise-elimination process. 952 windows were generated through feature extraction. To see the stress detection performance seven typical learning-based classifiers were used [5],[14]. They are: Decision tree, Random forest, Adaboosting, k nearest neighbor, Linear discriminant, Support Vector Machine(SVM), and gradient boosting. To compare performance between the existing method and the proposed method we used accuracy. And to measure the proposed method's performance the area under the receiver operating characteristic curve (AUC) [6] and F1 scores were used.

### 4.2 Integrated Approach Performance

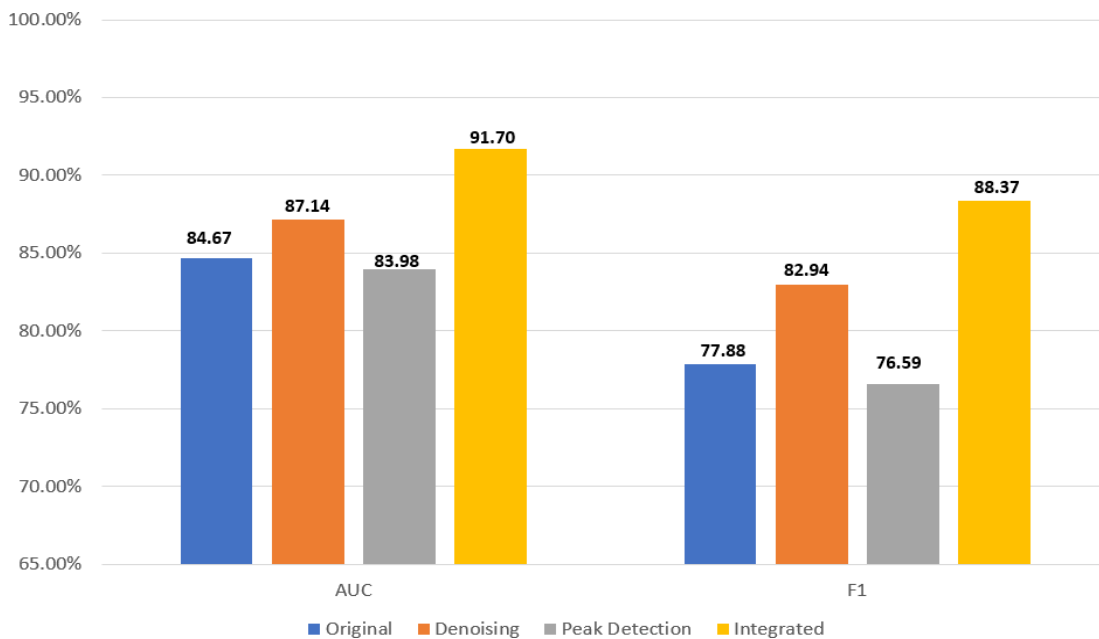


Figure 4.1: Performance results of the methods

We investigated the performance of the proposed integrated method by comparing it with the non-integrated methods: original, denoising without peak-detection, and ensembled peak-detection without denoising. We used the average of five peak-detection methods for denoising without a peak-detection method. Figure 4.1 shows the result by averaging all the results of the seven classifiers of AUC and F1 score. We can see that the integrated method has the best performance with a result of 91.70 for AUC and 88.37 for the F1 score. It is more than 4.43% for AUC and 5.01% for the F1 score compared with the second best option. The Second best option is a two-step denoising method. Peak detection without denoising had the lowest performance because it was applied on low-quality signals that contained a lot of noise. Thus, the integrated method achieved better performance than any of the other methods.

TABLE 2. Performance comparison between the proposed method and existing method

|                  | Decision tree      | Random Forest | Ada-boosting | KNN(K=9)     | LDA          |
|------------------|--------------------|---------------|--------------|--------------|--------------|
|                  | Accuracy(F1 score) |               |              |              |              |
| Philip, et al[9] | 81.39(78.27)       | 84.18(81.35)  | 84.10(81.23) | 82.06(78.94) | 85.83(83.08) |
| Our's            | 90.75(86.54)       | 91.57(87.47)  | 91.62(87.91) | 88.11(88.10) | 94.79(90.59) |

Table 2 presents the performance comparison between the existing method proposed by Schmidt, Philip, *et al* under the same conditions [9] and our integrated method. We measured the accuracy and F1 score using the same approach adopted in the previous method. The five classifiers demonstrated that our one outperforms the previous method by achieving a performance improvement at an average accuracy of 7.86% and F1 score of 7.80%.

TABLE 3. Summary of the performance of the integrated method with seven classifiers

|     | Decision tree | Random forest | Ada-boosting | KNN (k=9) | LDA   | Support Vector Machine(SVM) | Gradient boosting | Average |
|-----|---------------|---------------|--------------|-----------|-------|-----------------------------|-------------------|---------|
| AUC | 90.32         | 90.74         | 90.99        | 92.20     | 93.11 | 92.28                       | 91.59             | 91.70   |
| F1  | 86.54         | 87.47         | 87.91        | 88.10     | 90.59 | 88.99                       | 88.99             | 88.37   |

Table 3 presents the results of each classifier. This table lists the AUC and F1 scores of each of the seven classifiers. The Linear discriminant analysis (LDA) classifier achieved the best result with 93.11 for AUC and 90.59 for the F1 score.

### 4.3 Two-Step denoising method performance

At first we measured the performance of the original signal. Then we only filtered the noise and measured the performance. Finally, we applied noise elimination to that filtered noise to see the effect of two-step denoising. In every step, we have used ensemble-based peak detecting methods.

Figure 4.2 shows the two-step denoising method performance result by averaging all the results of the seven classifiers of AUC and F1 scores. The two-step denoising method has the best result with 91.70 for AUC and 88.37 for the F1 score which is increased by 1.96% for AUC and 2.54% for the F1 score compared with only noise filtering. An increase in performance of 7.03% for AUC and 10.49% for the F1 score compared with the worst option that did not use any of the denoising methods was also achieved.

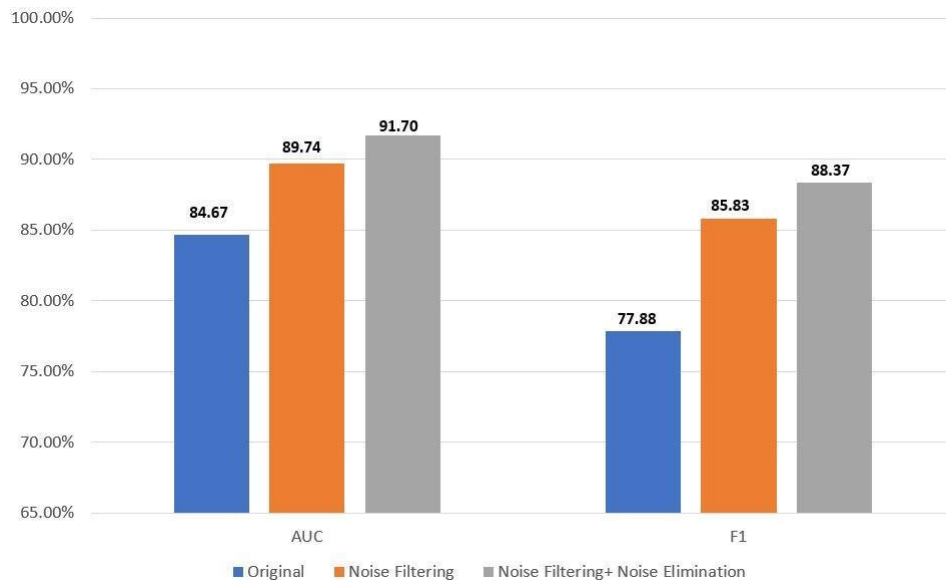


Figure 4.2: Performance of two-step denoising method with ensembled peak detection method

## 4.4 Ensemble-based peak detection performance

To compare the peak detection methods' performance we use 5 different peak detection methods and then ensemble them. These 5 methods are - Local maxima method (LMM), Block generation with the mean of the signal threshold method (BGM), First derivative with an adaptive threshold method (FDA), Slope sum function with an adaptive threshold method (SFA), Moving averages with the dynamic threshold method (MAD). We have applied these methods after noise filtering and elimination of the signal. In table 4, we can see the peak detection methods performance result by averaging all the results of the seven classifiers of AUC and F1 scores. Ensemble-based peak detection method has the best result with 91.70% for AUC and 88.37% for the F1 score.

TABLE 4. Summary of the performance of peak detecting methods with seven classifiers

| Peak-detecting method | Decision Tree  | Random forest | Adaboosting   | KNN (k=9)     | LDA           | SVM           | Gradient boosting | Average       |
|-----------------------|----------------|---------------|---------------|---------------|---------------|---------------|-------------------|---------------|
|                       | AUC (F1 score) |               |               |               |               |               |                   |               |
| LMM                   | 78.68 (67.15)  | 82.83 (74.38) | 81.86 (72.27) | 81.39 (70.50) | 81.55 (70.60) | 84.60 (76.48) | 83.94 (76.01)     | 82.12 (72.48) |
| BGM                   | 86.42 (81.43)  | 88.50 (83.44) | 91.28 (87.72) | 89.73 (84.11) | 92.08 (89.13) | 91.30 (87.30) | 90.32 (86.94)     | 89.94 (85.72) |
| FDA                   | 87.47 (81.04)  | 89.14 (84.47) | 88.93 (83.71) | 90.34 (85.37) | 92.07 (88.03) | 91.18 (86.99) | 90.99 (86.71)     | 90.06 (85.19) |
| SFA                   | 82.48 (74.44)  | 87.47 (81.77) | 88.69 (83.07) | 87.36 (81.19) | 91.65 (87.81) | 91.49 (87.39) | 89.34 (83.97)     | 88.35 (82.80) |
| MAD                   | 85.35 (78.34)  | 89.02 (84.62) | 88.37 (84.06) | 90.79 (86.99) | 93.81 (91.18) | 92.69 (89.36) | 91.58 (87.66)     | 90.23 (86.03) |
| ENS.                  | 90.32 (86.54)  | 90.74 (87.47) | 90.99 (87.91) | 92.21 (88.10) | 93.22 (90.59) | 92.83 (88.99) | 91.59 (88.99)     | 91.70 (88.37) |

# Chapter 5

## Conclusion And Future work

### 5.1 Conclusion

In this research, we have implemented a two-step denoising and ensemble-based peak-detection method together to improve stress detection performance. This integrated method demonstrated superior stress-detection performance over the existing method with multiple classifiers. We have also explored the result before and after using the denoising methods in the PPG signal. The integrated method gives better performance. Now different denoising methods should be applied to see whether they can provide a better result than this.

### 5.2 Future Work

We have used Fourier Transformation (FFT) to denoise the PPG signal and got experimental results as regards. We have done some research on this topic and found out that Wavelet Transform does better in low amplitude signals than Fourier Transform. It is also more efficient in dealing with time-frequency analysis than Fourier transform. In the future, We will implement this Wavelet Transformation instead of it and will explore whether it actually provides an improved result or not.

# References

- [1] T. Fawcett, "An introduction to ROC analysis," Pattern Recognit. Lett., vol. 27, no. 8, pp. 861-874, Jun. 2006, doi:<https://doi.org/10.1016/j.patrec.2005.10.010>
- [2] P. V. Kasambe, and S. S. Rathod, "VLSI wavelet based denoising of PPG signal." Procedia Computer Science, vol. 49, pp. 282-288, 2015, doi:<https://doi.org/10.1016/j.procs.2015.04.254>
- [3] B. Mishra and N. S. Nirala, "A Survey on Denoising Techniques of PPG Signal," 2020 IEEE International Conference for Innovation in Technology (INOCON), pp. 1-8, 2020, doi:<https://doi.org/10.1109/INOCON50539.2020.9298358>.
- [4] K. KAVITHA, S. VASUKI, and B. KARTHIKEYAN, "PPG Signal Denoising using a New Method for the Selection of Optimal Wavelet Transform Parameters," Journal of University of Shanghai for Science and Technology, vol. 23, Oct 21.
- [5] J. Zhai and A. Barreto, "Stress detection in computer users through noninvasive monitoring of physiological signals," Biomed Sci Instrum, vol. 42, pp. 495-500, 2006, PMID:16817657.
- [6] K. A. Reddy, B. George and V. J. Kumar, "Use of Fourier Series Analysis for Motion Artifact Reduction and Data Compression of Photoplethysmographic Signals," in IEEE Transactions on Instrumentation and Measurement, vol. 58, no. 5, pp. 1706-1711, May 2009, doi:<https://doi.org/10.1109/TIM.2008.2009136>.
- [7] M. Elgendi, I. Norton, M. Brearley, D. Abbott, D. Schuurmans, "Systolic peak detection in acceleration photoplethysmograms measured from emergency responders in tropical conditions," PLoS One, vol. 8, Oct 22 2013, doi:<https://doi.org/10.1371/journal.pone.0076585> PMID:24167546; PMCID: PMC3805543.
- [8] A. Alqaraawi, A. Alwosheel, and A. Alasaad, "Heart rate variability estimation in photoplethysmography signals using Bayesian learning approach," Healthcare technology letters, vol. 3(2), pp. 136-142, Jun 2016, doi: <https://doi.org/10.1049/htl.2016.0006>
- [9] P. Schmidt, A. Reiss, R. Duerichen, C. Marberger, and K. Van Laerhoven, "Introducing WESAD, a multimodal dataset for wearable stress and affect detection," in Proc. 20th ACM Int. Conf. Multimodal Interact., pp. 400-408, Oct. 2018, doi:<https://doi.org/10.1145/3242969.3242985>
- [10] S. Heo, I. Kim, S. Kwon, H. Lee, and J. Lee, "PPG signal preprocessing and comparison study with learning-based model for stress detection," J. Korean Inst. Commun. Sci., pp. 595-596, Aug. 2020.

- [11] S. Heo, S. Kwon and J. Lee, "Stress Detection With Single PPG Sensor by Orchestrating Multiple Denoising and Peak-Detecting Methods," in IEEE Access, vol. 9, pp. 47777-47785, 2021, doi: <https://doi.org/10.1109/ACCESS.2021.3060441>.
- [12] E. Harikrishna, and K. A. Reddy, "Use of Transforms in Biomedical Signal Processing and Analysis", in Real Perspective of Fourier Transforms and Current Developments in Superconductivity. London, United Kingdom: IntechOpen, May, 2021. doi: <https://doi.org/10.5772/intechopen.98239>
- [13] Yi-Hsiang Yang and Kea-Tiong Tang, "A pulse oximetry system with motion artifact reduction based on Fourier analysis," 2014 IEEE International Symposium on Bioelectronics and Bioinformatics (IEEE ISBB 2014), 2014, pp. 1-4, doi: <https://doi.org/10.1109/ISBB.2014.6820902>.
- [14] A. Esmaili, M. Kachuee and M. Shabany, "Nonlinear Cuffless Blood Pressure Estimation of Healthy Subjects Using Pulse Transit Time and Arrival Time," in IEEE Transactions on Instrumentation and Measurement, vol. 66, no. 12, pp. 3299-3308, Dec. 2017, doi: <https://doi.org/10.1109/TIM.2017.2745081>.
- [15] S. S. Bashar, M. S. Miah, A. H. M. Z. Karim and M. A. Al Mahmud, "Extraction of Heart Rate from PPG Signal: A Machine Learning Approach using Decision Tree Regression Algorithm," 2019 4th International Conference on Electrical Information and Communication Technology (EICT), 2019, pp. 1-6, doi: <https://doi.org/10.1109/EICT48899.2019.9068845>
- [16] Islam, M.T., Ahmed, S.T., Shahnaz, C. et al. "SPECMAR: fast heart rate estimation from PPG signal using a modified spectral subtraction scheme with composite motion artifacts reference generation," Med Biol Eng Comput 57, pp. 689–702 ,2019. doi: <https://doi.org/10.1007/s11517-018-1909-x>
- [17] D. Ban and S. Kwon, "Movement noise cancellation in PPG signals," 2016 IEEE International Conference on Consumer Electronics (ICCE), 2016, pp. 47-48, doi: <https://doi.org/10.1109/ICCE.2016.7430517>.
- [18] K. V. P. Narahariseti and M. Bawa, "Comparison of different signal processing methods for reducing artifacts from photoplethysmograph signal," 2011 IEEE INTERNATIONAL CONFERENCE ON ELECTRO/INFORMATION TECHNOLOGY, 2011, pp. 1-8, doi: <https://doi.org/10.1109/EIT.2011.5978571> .